CRISPR BIOLOGY

A phage-encoded anti-CRISPR enables complete evasion of type VI-A CRISPR-Cas immunity

Alexander J. Meeske[1]*, Ning Jia[2]*, Alice K. Cassel[1], Albina Kozlova[1], Jingqiu Liao[3,4], Martin Wiedmann[3,4], Dinshaw J. Patel[2]†, Luciano A. Marraffini[1,5]†

The CRISPR RNA (crRNA)–guided nuclease Cas13 recognizes complementary viral transcripts to trigger the degradation of both host and viral RNA during the type VI CRISPR-Cas antiviral response. However, how viruses can counteract this immunity is not known. We describe a listeriaphage (ϕLS46) encoding an anti-CRISPR protein (AcrVIA1) that inactivates the type VI-A CRISPR system of *Listeria seeligeri*. Using genetics, biochemistry, and structural biology, we found that AcrVIA1 interacts with the guide-exposed face of Cas13a, preventing access to the target RNA and the conformational changes required for nuclease activation. Unlike inhibitors of DNA-cleaving Cas nucleases, which cause limited immunosuppression and require multiple infections to bypass CRISPR defenses, a single dose of AcrVIA1 delivered by an individual virion completely dismantles type VI-A CRISPR-mediated immunity.

CRISPR-Cas systems are prokaryotic adaptive immune systems that protect their hosts from invasion by viruses (*1*) and plasmids (*2*). CRISPR loci contain short DNA repeats separated by spacer sequences of foreign origin (*3–5*). To achieve immunity, the locus is transcribed and processed into small CRISPR RNAs (crRNAs), which associate with RNA-guided Cas nucleases (*6*) to locate and cleave complementary nucleic acid sequences (protospacers) (*7*). CRISPR systems are categorized into six types (I to VI) that differ in their *cas* gene content and mechanism of immunity (*8*). Although most types neutralize invaders through destruction of their DNA, Cas13, the RNA-guided nuclease of type VI systems, unleashes nonspecific RNA degradation (*trans*-RNase activity) upon recognition of a phage target transcript (*9–11*). The cleavage of host transcripts leads to a growth arrest that prevents further propagation of the phage, allowing the uninfected cells in the population to survive and proliferate (*11*). Because the phage genome is not directly affected by Cas13, it continues to produce target transcripts, leading to a persistent activation of the nuclease and to growth arrest (*11*).

Identification of the Cas13a inhibitor AcrVIA1

Presumably in response to the pressure imposed by CRISPR-Cas immunity, phages evolved anti-CRISPR (Acr) proteins, small proteins (usually <150 amino acids) that are produced during infection and inactivate Cas nucleases (*12*). Acrs also exhibit exceptional diversity of sequences and mechanisms and, with few exceptions, specifically inhibit one CRISPR subtype (*12–17*). Recently, inhibitors of Cas13a were independently reported (*18*); however, how they allow phages to overcome the type VI-A CRISPR-Cas response is not known. To investigate the molecular mechanisms used by Acr-carrying phages to inhibit Cas13 during infection of a natural host, we first obtained temperate phages from a collection of 62 environmental isolates of *Listeria* spp., an organism that commonly harbors type VI-A CRISPR-Cas systems. We induced prophages with mitomycin C and isolated phages that infected a mutant of *Listeria seeligeri* SLCC3954 (*19*) lacking its two restriction-modification (RM) systems and the type VI-A CRISPR array (*L. seeligeri* ΔRM Δ*spc*; fig. S1A). We isolated 15 phages (fig. S1B), which we used to infect wild-type (WT) *L. seeligeri*, and obtained 10 lysogens carrying different prophages in their genomes (fig. S1C). We then tested each lysogen for its ability to disable Cas13a-mediated immunity against plasmid conjugation (fig. S1D). Only the ϕLS46 lysogen exhibited a high efficiency of plasmid transfer (Fig. 1A and fig. S1D), suggesting the possibility that this prophage harbors a Cas13a inhibitor.

Sequencing of the ϕLS46 genome revealed an organization similar to a previously characterized temperate phage of *L. seeligeri*, ϕRR4 (*11*), which harbors an anti-CRISPR region containing six genes, two of them with homology to the Cas9 inhibitors AcrIIA1 and AcrIIA2 (fig. S1E). In ϕLS46, however, this region contains four genes, none of which displayed strong homology to known inhibitors (Fig. 1B and fig. S1E). To investigate whether this region contains a type VI Acr, we cloned the operon with its native promoter into a plasmid (p*gp1-4*), introduced it into WT *L. seeligeri*, and tested for Cas13a-mediated immunity against plasmid conjugation. Indeed, the presence of p*gp1-4* allowed plasmid conjugation even in the presence of Cas13a targeting, and cloning each individual gene allowed us to identify *gp2* as the gene responsible for this anti-CRISPR phenotype (Fig. 1C). Accordingly, we renamed *gp2* "type VI-A anti-CRISPR 1," or AcrVIA1 ($AcrVIA1^{Lse}$ to distinguish from other genes). AcrVIA1 is a protein of 232 amino acids, considerably larger than most previously discovered Acrs. Gp1, AcrVIA1, and Gp4 exhibit no detectable homology to proteins of known function, but we noted that Gp3 contains a helix-turn-helix (HTH) domain with limited similarity to AcrIIA6 from *Streptococcus* phage DT1, suggesting that it may be an inhibitor of type II-A CRISPR-Cas systems. Many listeriaphages harbor the HTH-containing AcrIIA1, which serves dual roles as an Acr and as a transcription autorepressor of the *acr* cassette during late lytic infection (*20*). To test whether Gp3 plays a similar role in ϕLS46, we fused the *acrVIA1* promoter to a *lacZ* reporter and measured β-galactosidase activity in the presence and absence of p*gp3* (fig. S2). We observed an ~10-fold reduction in transcription from the *acr* promoter in the presence of Gp3, a result that confirmed its role as a regulator of AcrVIA1 expression.

Next, we investigated whether AcrVIA1 was necessary for inhibition of Cas13a during ϕLS46 infection. We created a derivative of the ΔRM Δ*spc* strain in which we ectopically integrated different spacer sequences, with their transcription controlled by the native CRISPR promoter (strain ΔRM Ω*spcX*; fig. S1A). First, we inserted spacers targeting transcripts of either a conjugative plasmid or phage ϕLS59, the genome of which lacks *acr* genes, and confirmed that they could provide efficient immunity in this experimental system (fig. S3, A and B). We then cloned 10 spacers targeting different transcript regions of ϕLS46 (fig. S3C), none of which conferred immunity (fig. S3D). Finally, we isolated phage mutants in the Acr region of ϕLS46 and tested the same spacers for immunity against them. Although none of the spacers protected against WT ϕLS46, both the Δ*gp1-4* and Δ*acrVIA1* mutants exhibited one to six orders of magnitude higher sensitivity to Cas13a interference compared with a nontargeting control (Fig. 1D and fig. S3D). We expressed AcrVIA1 using the p*gp2* plasmid and found that it inhibited targeting of the Cas13a-susceptible phage ϕLS59 (Fig. 1E). Finally, the inhibition of antiplasmid immunity observed in the WT(ϕLS46) lysogen was abolished when we performed the conjugation assay using the WT(ϕLS46 Δ*acrVIA1*) lysogen (Fig. 1A). To explore the effect of AcrVIA1 on the Cas13a-induced host cell dormancy that is fundamental for type VI-A immunity, we induced the expression of *spc4* target RNA, which was previously shown to cause a severe growth defect as a result of nonspecific host transcript degradation (*11*). Expression of the inhibitor

[1]Laboratory of Bacteriology, The Rockefeller University, New York, NY 10065, USA. [2]Structural Biology Program, Memorial Sloan Kettering Cancer Center, New York, NY 10065, USA. [3]Department of Food Science, Cornell University, Ithaca, NY 14583, USA. [4]Graduate Field of Microbiology, Cornell University, Ithaca, NY 14583, USA. [5]Howard Hughes Medical Institute, The Rockefeller University, New York, NY 10065, USA.
*These authors contributed equally to this work.
†Corresponding author. Email: marraffini@rockefeller.edu (L.A.M.); pateld@mskcc.org (D.J.P.)

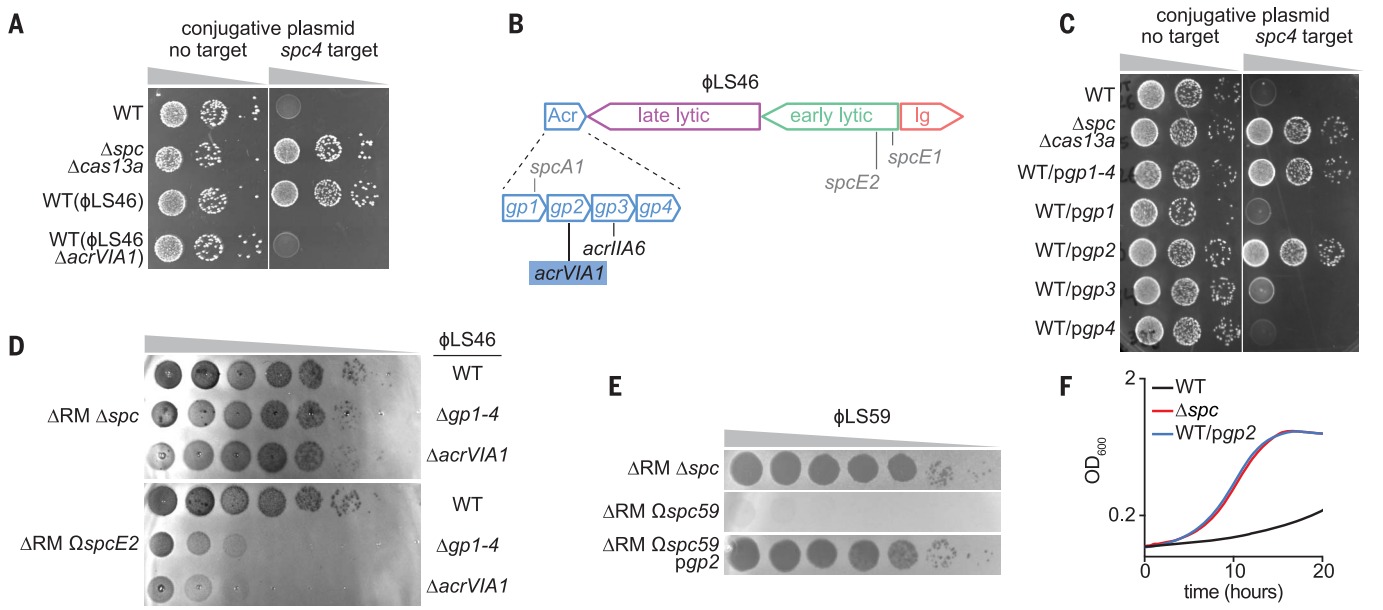

Fig. 1. AcrVIA1 inhibits type VI-A CRISPR-Cas immunity against plasmids and phages. (**A**) Transfer of a conjugative plasmid with or without the *spc4* target of the *L. seeligeri* type VI-A CRISPR-Cas system into different strains: WT, Δ*spc* Δ*cas13a*, or WT harboring the ϕLS46 or ϕLS46 Δ*acrVIA1* prophages. (**B**) Schematic of the ϕLS46 genome showing the four main transcription units (*acr*, lysogeny, and early- and late-lytic genes). *gp2* was renamed *acrVIA1*. The locations of the targets of spacers used in this study are shown in gray. (**C**) Same as (A) but using strains carrying plasmids to express different *acr* genes from ϕLS46. (**D**) Detection of phage propagation after spotting 10-fold dilutions of WT, Δ*gp1-4*, or Δ*acrVIA1* phage ϕLS46 on lawns of *L. seeligeri* ΔRM Δ*spc* or ΔRM Ω*spcE2*. (**E**) Same as (D) but spotting ϕLS59 into lawns of *L. seeligeri* ΔRM Δ*spc*, ΔRM Ω*spc59*, or ΔRM Ω*spc59/pgp2*. (**F**) Growth of WT, Δ*spc*, and WT/*pgp2* *L. seeligeri* strains expressing an *spc4* target RNA under the control of an anhydrotetracycline-inducible promoter after the addition of the inducer.

using the p*gp2* plasmid, however, reverted this growth defect (Fig. 1F). Thus, *acrVIA1* is necessary and sufficient to inhibit Cas13a-induced growth arrest and thereby thwart type VI CRISPR immunity against plasmids and phages.

AcrVIA1 binds Cas13a and inhibits *cis*- and *trans*-RNase activities

The inhibition of Cas13a-induced growth arrest suggested that AcrVIA1 could inhibit the *trans*-RNase activity of Cas13a. To investigate this, we purified both proteins (fig. S4, A and B) and tested their activities using in vitro RNA protospacer cleavage assays. A radiolabeled target RNA was used to investigate inhibition of Cas13a's *cis*-RNase activity. Purified *L. seeligeri* Cas13a^{crRNA} catalyzed rapid RNA cleavage of protospacer RNA, and this activity was gradually decreased in the presence of increasing concentrations of AcrVIA1 (Fig. 2, A and B). Similarly, AcrVIA1 inhibited Cas13a-mediated *trans*-cleavage of a labeled nontarget RNA upon addition of unlabeled protospacer RNA (Fig. 2C). To look for an interaction between the nuclease and its inhibitor, we added C-terminal hexahistidine and 3xFLAG tags to Cas13a and AcrVIA1, respectively, and confirmed that both were functional in *L. seeligeri* (fig. S4C) and in vitro (Fig. 2, A and C). We expressed Cas13a-His6 either alone or in the presence of AcrVIA1-3xFLAG and then performed immunoprecipitation with anti-Flag antibody resin. Analysis of the input, unbound, and immunoprecipitated fractions by immunoblot using antibodies against His6, FLAG, and the *L. seeligeri* housekeeping sigma factor σ^A as a control showed a specific coimmunoprecipitation of Cas13a-His6 with AcrVIA1-3xFLAG (Fig. 2D). Finally, we investigated whether the interaction of AcrVIA1 with Cas13a prevents binding of the Cas13a^{crRNA} complex to its complementary target RNA. To test this, we performed an electrophoretic mobility shift assay (EMSA) to measure the association of labeled protospacer RNA with a nuclease-dead dCas13a^{crRNA} complex (Fig. 2E). In the presence of this complex, most of the target RNA was shifted to multiple higher-molecular-weight species: one corresponding to a crRNA-protospacer RNA duplex and higher species representing the dCas13a^{crRNA}-protospacer ternary complex. By contrast, in the presence of equimolar AcrVIA1, the target RNA remained mostly unbound and unassociated with dCas13a^{crRNA}. Collectively, these results indicate that AcrVIA1 forms a complex with Cas13a^{crRNA} that prevents binding of the complementary target RNA and therefore inhibits both its *cis*- and *trans*-RNase activities.

Structure of the AcrVIA1-Cas13a^{crRNA} complex

To further investigate how AcrVIA1 suppresses Cas13a^{crRNA} activity, we isolated a stable homogeneous AcrVIA1-Cas13a^{crRNA} complex (fig. S5) and determined its cryo–electron microscopy (cryo-EM) structure, along with that of Cas13a^{crRNA} alone, at 3.0- and 3.2-Å resolution, respectively (fig. S6 and table S1). Cas13a^{crRNA} adopts a bilobed architecture, consisting of recognition [REC; N-terminal domain (NTD) and Helical-1 domain] and nuclease (NUC; Helical-2 and two HEPN domains connected by a Linker element) lobes (Fig. 3, A and C), similar to previously reported structures of Cas13a from other species (*21*, *22*). The complex contained a natural 51-nucleotide mature crRNA, which was processed and loaded in the native host (Fig. 3B and fig. S7A). Nucleotides 8 to 12 and 13 to 19 in the crRNA spacer region adopted an approximately A-form helical conformation, with their outward direction positioned to pair with the target RNA (fig. S7B), a feature different from the crRNA alignment in *Leptotrichia buccalis* Cas13a (*22*). The 5′ end of the repeat is located in the cleft between the Helical-1 and HEPN-2 domains (fig. S7A). Mutations in residues within this region of Cas13a (R1048A, K1049A) abrogate type VI interference against plasmid conjugation (fig. S7C), revealing their importance for crRNA maturation.

In the AcrVIA1-Cas13a^{crRNA} complex, the inhibitor is positioned on the crRNA-exposed face of Cas13a and directly interacts with the crRNA and residues in the Helical-1, NTD, HEPN-1, and Linker domains of Cas13a (Fig. 3,

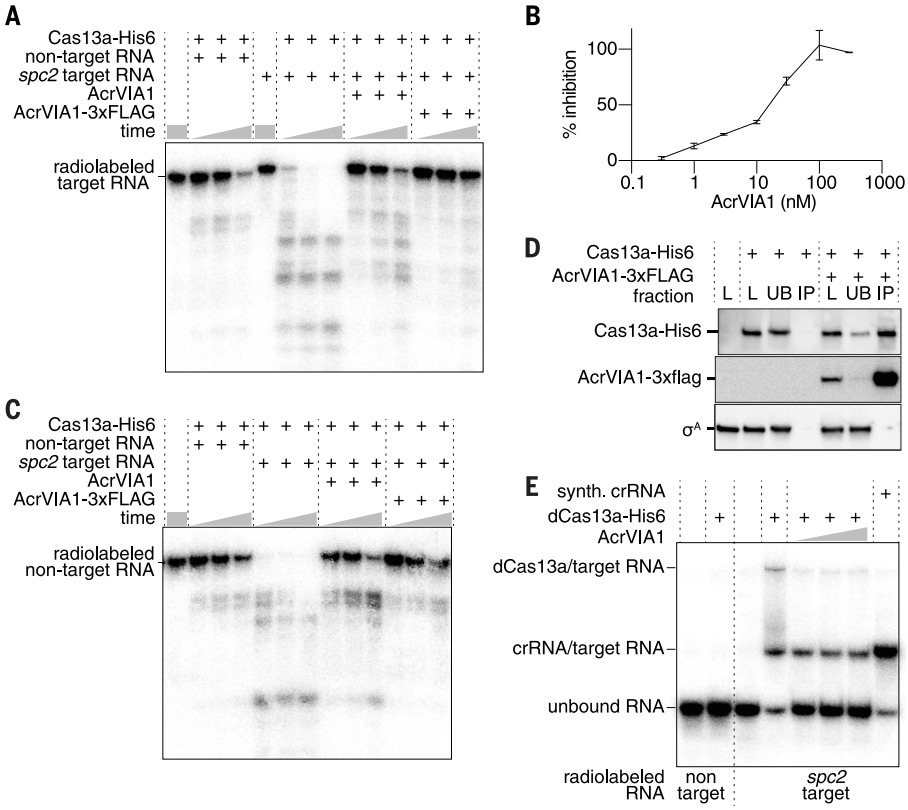

Fig. 2. AcrVIA1 interacts with Cas13a^{crRNA} to prevent binding of the target RNA and RNase activation. (**A**) *cis*-RNA cleavage time course with purified *L. seeligeri* Cas13a-His6, AcrVIA1, and/or AcrVIA1-3xFLAG using radiolabeled nontarget or *spc2*-target RNA substrates. Reactions were analyzed after 5, 10, or 20 min of incubation. (**B**) Dose response of Cas13a cis-RNase inhibition by AcrVIA1-3xFLAG. (**C**) *trans*-RNA cleavage time course as in (A) but using a radiolabeled nontarget RNA substrate in the presence of unlabeled nontarget or *spc2*-target RNA. (**D**) Anti-FLAG immunoprecipitation using protein extracts from *L. seeligeri* cells expressing either Cas13a-His6 alone or coexpressing AcrVIA1-3xFLAG. The His6 and FLAG epitopes and the σ^A protein were detected by immunoblot. (**E**) EMSA of radiolabeled nontarget or *spc2*-target RNAs in the presence of dCas13a-His6, with 2:1, 1:1, or 1:2 equivalents of AcrVIA1-3xFLAG.

D to H, and fig. S8, A to D), with a buried interface area of ~1800 Å^2. There is no structural similarity between AcrVIA1 and other reported structures according to a DALI search (*23*), indicating a new fold for this inhibitor. Residues in AcrVIA1 form extensive hydrophobic and hydrophilic interactions with the crRNA, which has been shown previously to undergo large conformational changes, especially at its 3′ end, upon target RNA binding to activate Cas13a RNase activity (*22*). Notably, the 3′ end of the crRNA in the AcrVIA1-Cas13a^{crRNA} complex is stabilized by hydrogen bonds formed by N43, S40, and S93 and stacking interactions between U21 in crRNA and Y39 and V94 in AcrVIA1 (Fig. 3F), F69 stacks on A17 in the middle spacer region of crRNA (Fig. 3G), and F103 stacks on U27 in the 5′ repeat region of crRNA (Fig. 3E). In addition, the acidic loop E131 to E134 in the inhibitor points toward and blocks access to the central C13 to A17 region of the crRNA (Fig. 3G). This region has been shown previously to be critical for target RNA binding and to turn on Cas13a RNase activity (*9*, *22*).

AcrVIA1 also interacts directly with Cas13a, making several intermolecular contacts in the complex. Residues S93, Q96, and I97 in the inhibitor form hydrogen bonds with N259 and K261 in the Helical-1 domain of the nuclease (Fig. 3F), and residue F69 in AcrVIA1 stacks on R310 of the same domain (Fig. 3G). S68 in AcrVIA1 forms hydrogen bonds with R90 in the NTD domain (Fig. 3G), whereas residues I2 and Y4 in the inhibitor stack on K1097 in the HEPN-1 domain (Fig. 3H). The two C-terminal helices of AcrVIA1 form extensive interactions with the Linker domain of Cas13a, locking it in place (Fig. 3H) and thereby preventing the conformational changes reported to occur upon target RNA binding (*22*). Finally, we detected only minimal structural changes of Cas13a upon AcrVIA1 binding (fig. S9A). By contrast, the 3′ end of crRNA underwent a large conformational rearrangement (fig. S9, B and C). Thus, AcrVIA1 prevents conformational changes in the crRNA that occur upon target RNA binding, which are required for activation of Cas13a. To investigate the importance of the observed contacts between the nuclease and its inhibitor, we mutated the relevant residues in AcrVIA1-3xFLAG and tested their importance in inhibiting Cas13a immunity against plasmid conjugation (Fig. 3I), as well as their impact on protein stability by immunoblot (Fig. 3J). Mutations in I2A or Y4A or deletion of the E131 to E134 loop affected both the stability and the function of the inhibitor. By contrast, the quintuple mutant Y39A, S40A, N43A, S93A, Q96A and the truncation mutant lacking the two AcrVIA1 C-terminal helices (ΔN173-N232) caused nearly complete loss of function with little or no effect on protein expression, corroborating their importance for Cas13a inhibition. When tested individually, none of the five substitutions affected inhibition (fig. S7D), a result that suggests a very strong association between AcrVIA1 and Cas13a that does not rely on a single interaction. The S68A, F69A double mutant retained full function, suggesting that the interaction with Cas13a is unperturbed in this mutant. However, the mutation also led to an increase in expression levels, which could compensate for a partial loss of function.

AcrVIA1 had no effect on protospacer RNA cleavage by purified *L. buccalis* Cas13a^{crRNA} (fig. S10A). We performed a structural comparison of *L. seeligeri* Cas13a with *L. buccalis* Cas13a (PDB 5XWY). Superposition of *L. seeligeri* Cas13a^{crRNA} and *L. buccalis* Cas13a^{crRNA} revealed differences in the NTD domain (fig. S10B) and the 3′ end of crRNA (fig. S10C) that generated obvious clashes between *L. buccalis* Cas13a^{crRNA} and AcrVIA1 (fig. S10, D and E). In addition, there were no identifiable overall structural similarities with the other subtype family members Cas13b (*24*, *25*) or Cas13d (*26*). Thus, our structural analysis and biochemical tests suggest that AcrVIA1 is limited to neutralizing only the *L. seeligeri* type VI-A CRISPR-Cas immune response.

AcrVIA1 enables complete evasion of type VI-A CRISPR-Cas immunity

Previously described anti-CRISPRs that inhibit type I and II CRISPR systems require multiple rounds of infection to completely inhibit antiphage immunity and fail in conditions of strong CRISPR defense or low viral load (*27*, *28*). To investigate whether AcrVIA1 also displayed limited inhibition capabilities, we first tested its efficacy in conditions of weak or strong type VI-A CRISPR-Cas immunity by infecting cells harboring either one or three targeting spacers, respectively (Fig. 1B). As a control, we performed infections with the ϕLS46 Δ*acrVIA1* mutant phage and measured the efficiency of plaquing (EOP) in the different host backgrounds. When compared with infection of hosts without targeting spacers, all three individual

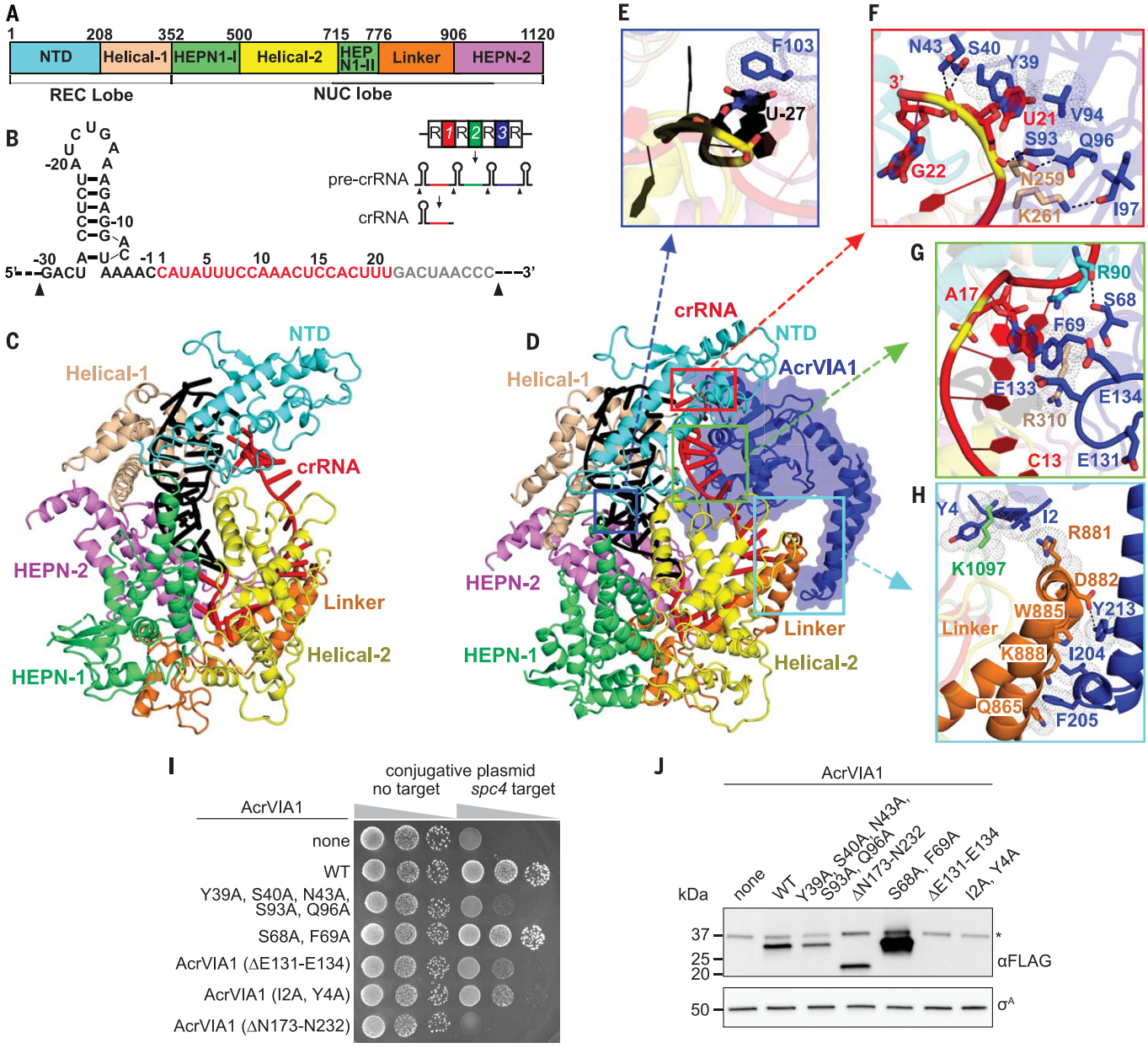

Fig. 3. Cryo-EM structures of Cas13a^{crRNA} and AcrVIA1-Cas13a^{crRNA} complexes. (**A**) Domain organization of *L. seeligeri* Cas13a. (**B**) Schematic representation of the crRNA sequence. The repeat and spacer regions within crRNA are shown in black and red, respectively. The disordered region is shown in gray. The black arrow shows the cleavage site of the pre-crRNA. Inset: crRNA maturation pathway; repeats are represented as "R" and spacers as numbers. (**C**) Ribbon representation of the structure of Cas13a^{crRNA}. (**D**) Ribbon and surface (AcrVIA1) representations of AcrVIA1-Cas13a^{crRNA} complex. (**E** to **H**) Detailed interactions between AcrVIA1 and Cas13a^{crRNA} in the complex. (**I**) Transfer of conjugative plasmid with or without the *spc4* target of the *L. seeligeri* type VI CRISPR-Cas system into WT *L. seeligeri* harboring plasmid-borne WT or mutant alleles of *acrVIA1-3xflag*. (**J**) Anti-Flag immunoblot of AcrVIA1 mutants tested in (I) and an anti-σ^A loading control. *Cross-reacting protein.

spacers as well as the triple combination provided efficient immunity against this mutant, reducing the EOP by at least eight orders of magnitude, below our limit of detection. By contrast, immunity was completely abrogated (~100% EOP) during infections with WT ϕLS46 when plating on either the single-spacer or triple-spacer strains (Fig. 4A). The 100% EOP value obtained indicated that each viral particle was able to inhibit Cas13a and form a visible plaque. To test this further, we performed infection of liquid cultures of *L. seeligeri* ΔRM at an extremely low multiplicity of infection (MOI), 0.000001, and followed their growth over time. In the absence of a targeting spacer, both WT and Δ*acrVIA1* mutant phage led to the lysis of the bacteria in the culture (Fig. 4B). Although *L. seeligeri* strains harboring a single ϕLS46-targeting spacer were immune to the Δ*acrVIA1* mutant phage, WT ϕLS46 was able to lyse the cultures (Fig. 4, C to E; figs. S3, C and D, and S11), showing that AcrVIA1 efficiently inhibits type VI-A CRISPR immunity even in conditions of low MOI. Infection of the strain containing three targeting spacers resulted in a delay in lysis (Fig. 4F), consistent with the stronger immunity provided by the presence

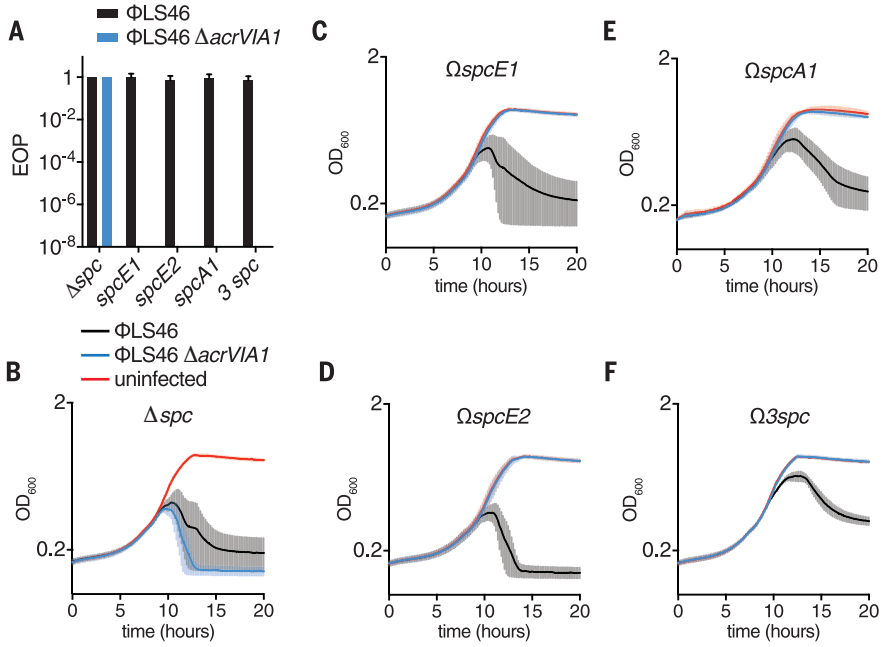

Fig. 4. AcrVIA1 enables full phage escape from type VI-A CRISPR-Cas immunity. (**A**) Efficiency of plaquing (relative to the number of plaques formed in lawns of *L. seeligeri* ΔRM Δ*spc*) of phages ϕLS46 or ϕLS46 Δ*acrVIA1* in lawns of bacteria expressing *spcA1*, *spcE1*, *spcE2*, or all three (*3spc*). Error bars represent SEM from three biological replicates. (**B** to **F**) Growth of *L. seeligeri* ΔRM Δ*spc* (B), ΔRM Ω*spcE1* (C), ΔRM Ω*spcE2* (D), ΔRM Ω*spcA1* (E), and ΔRM Ω3*spc* (F), measured as optical density at 600 nm (OD_{600}) over time after infection with ϕLS46 or ϕLS46 Δ*acrVIA1* phages or no infection. The average curves of three different replicates are reported, with ± SEM values shown.

of multiple spacers, yet still led to inhibition of the type VI-A CRISPR immune response. To explore the mechanism of inhibition further, we performed RNA sequencing over the course of ϕLS46 infection to determine the timing and expression of each protospacer. We found that many of the spacers used in this study targeted phage transcripts that were abundantly produced within 10 min of infection (e.g., those targeted by *spcA1*, *spcE1*, and *spcE2*; fig. S12) yet were unable to provide Cas13a-mediated immunity in the presence of AcrVIA1. Thus, AcrVIA1 overcame immunity against protospacers transcribed very early (even earlier than the inhibitor itself, as in the case of target A1) during the phage lytic cycle. Altogether, these results demonstrate that AcrVIA1 can enable viral propagation in conditions that are extremely unfavorable for the success of Cas13a inhibition (rapid targeting, low MOI, and multiple Cas13a targeting spacers) that normally would lead to the failure of type I and II Acrs (*27*, *28*).

Discussion

AcrVIA1 inhibits Cas13a by interacting with the crRNA-exposed face of nuclease and making specific contacts with both protein and guide RNA residues that prevent the binding of a complementary target RNA and activation of Cas13a RNase function. In heterologous hosts, AcrVIA1 could be a useful component of the Cas13 toolbox, allowing control of this nuclease during editing, knockdown, and/or visualization of RNA molecules (*29*, *30*), as is the case for other recently found type VI-A anti-CRISPRs (*18*). More importantly, in its natural host, AcrVIA1 can completely neutralize type VI-A CRISPR-Cas immunity against ϕLS46 even in unfavorable conditions for inhibition, such as multiple protospacer targeting and low viral load. We believe this to be a consequence of the lack of phage DNA clearance during the type VI response (*11*). This would lead to a continuous transcription and translation of AcrVIA1 and progressive neutralization of Cas13a. Assuming that the collateral RNA degradation generated by activation of Cas13a in *Listeria* hosts allows a low level of AcrVIA1 transcription and translation, enough inhibitor will accumulate to inactivate all the Cas13a molecules inside the bacterial cell. This is in contrast to type I and II Acrs, the initial production of which inhibits only a fraction of Cascade-Cas3 and Cas9 molecules, respectively, and the Acr-harboring phage is destroyed by the nucleases that remain active (*27*, *28*). Gradual inhibition of Cas13a after phage infection would require AcrVIA1 to constantly capture the $Cas13a^{crRNA}$ molecules that disengage from the target RNA and prevent them from finding their targets again. Alternatively, the inhibitor could displace the target RNA molecules from activated $Cas13a^{crRNA}$ nucleases. Such a mechanism would be especially effective when the target RNA is a transcript that is produced, and therefore activates Cas13a, before AcrVIA1 is generated. Finally, the genetic, biochemical, and structural findings of this work highlight the astounding diversity of molecular strategies at play during the host-virus evolutionary arms race.

REFERENCES AND NOTES

1. R. Barrangou *et al.*, *Science* **315**, 1709–1712 (2007).
2. L. A. Marraffini, E. J. Sontheimer, *Science* **322**, 1843–1845 (2008).
3. A. Bolotin, B. Quinquis, A. Sorokin, S. D. Ehrlich, *Microbiology* **151**, 2551–2561 (2005).
4. F. J. Mojica, C. Díez-Villaseñor, J. García-Martínez, E. Soria, *J. Mol. Evol.* **60**, 174–182 (2005).
5. C. Pourcel, G. Salvignol, G. Vergnaud, *Microbiology* **151**, 653–663 (2005).
6. S. J. Brouns *et al.*, *Science* **321**, 960–964 (2008).
7. R. N. Jackson, P. B. van Erp, S. H. Sternberg, B. Wiedenheft, *Curr. Opin. Microbiol.* **37**, 110–119 (2017).
8. K. S. Makarova *et al.*, *Nat. Rev. Microbiol.* **18**, 67–83 (2020).
9. O. O. Abudayyeh *et al.*, *Science* **353**, aaf5573 (2016).
10. A. East-Seletsky *et al.*, *Nature* **538**, 270–273 (2016).
11. A. J. Meeske, S. Nakandakari-Higa, L. A. Marraffini, *Nature* **570**, 241–245 (2019).
12. J. Bondy-Denomy, A. Pawluk, K. L. Maxwell, A. R. Davidson, *Nature* **493**, 429–432 (2013).
13. B. J. Rauch *et al.*, *Cell* **168**, 150–158.e10 (2017).
14. A. Pawluk *et al.*, *Cell* **167**, 1829–1838.e9 (2016).
15. Y. Bhoobalan-Chitty, T. B. Johansen, N. Di Cianni, X. Peng, *Cell* **179**, 448–458.e11 (2019).
16. N. D. Marino *et al.*, *Science* **362**, 240–242 (2018).
17. K. E. Watters, C. Fellmann, H. B. Bai, S. M. Ren, J. A. Doudna, *Science* **362**, 236–239 (2018).
18. P. Lin *et al.*, *Mol. Cell* S1097-2765(20)30225-2 (2020).
19. J. Rocourt, A. Schrettenbrunner, H. Hof, E. P. Espaze, *Pathol. Biol. (Paris)* **35**, 1075–1080 (1987).
20. B. A. Osuna *et al.*, *Cell Host Microbe* S1931-3128(20)30191-8 (2020).
21. L. Liu *et al.*, *Cell* **170**, 714–726.e10 (2017).
22. L. Liu *et al.*, *Cell* **168**, 121–134.e12 (2017).
23. L. Holm, C. Sander, *Trends Biochem. Sci.* **20**, 478–480 (1995).
24. I. M. Slaymaker *et al.*, *Cell Rep.* **26**, 3741–3751.e5 (2019).
25. B. Zhang *et al.*, *Cell Res.* **28**, 1198–1201 (2018).
26. C. Zhang *et al.*, *Cell* **175**, 212–223.e17 (2018).
27. A. L. Borges *et al.*, *Cell* **174**, 917–925.e10 (2018).
28. M. Landsberger *et al.*, *Cell* **174**, 908–916.e12 (2018).
29. O. O. Abudayyeh *et al.*, *Nature* **550**, 280–284 (2017).
30. D. B. T. Cox *et al.*, *Science* **358**, 1019–1027 (2017).

ACKNOWLEDGMENTS

We thank all members of the Marraffini laboratory for helpful discussions, R. Calendar (UC Berkeley) for A118 and U153 listeriaphages, S. Kilcher (ETH Zürich) for plasmid pSK1, D. Rudner (Harvard Medical School) for anti-σ^A antibody, M. J. De La Cruz for assistance in data collection on the Sloan Kettering Titan KRIOS cryo-EM, and E. Eng (New York Structural Biology Center) for assistance in cryo-EM data processing. **Funding:** This work was supported by a National Institutes of Health Director's Pioneer Award (1DP1GM128184-01 to L.A.M.), funds from the Geoffrey Beene Cancer Research Center and NIH GM129430 to D.J.P., and by a Memorial Sloan-Kettering Cancer Center Core Grant (P30CA008748). L.A.M. is an investigator of the Howard Hughes Medical Institute. A.J.M. is a Helen Hay Whitney postdoctoral fellow. **Author contributions:** A.J.M. and L.A.M. conceived the study. A.J.M. performed all the in vivo and biochemistry experiments with the help of A.K.C. and A.K. N.J. performed all the cryo-EM experiments. J.L. and M.W. isolated *L. seeligeri* strains. A.J.M., N.J., L.A.M., and D.J.P. wrote the manuscript. All authors read and approved the manuscript. **Competing interests:** L.A.M. and A.J.M. are coinventors on a patent application filed by The Rockefeller University relating to work in this study. L.A.M. is a founder of and adviser for Intellia Therapeutics and Eligo Biosciences. **Data and materials**

availability: The *L. seeligeri* strains LS46 and LS59 draft genome assemblies have been deposited at GenBank (accession no. JAAIYQ000000000). Raw genome sequencing reads and RNA-sequencing reads have been deposited at the Sequence Read Archive (accession no. PRJNA607241). The atomic coordinates have been deposited in the Protein Data Bank with the codes 6VRC (Cas13a^{crRNA}) and 6VRB (AcrVIA1-Cas13a^{crRNA}). The cryo-EM density maps have been deposited in the Electron Microscopy Data Bank with the codes EMD-21367 (Cas13a^{crRNA}) and EMD-21366 (AcrVIA1-Cas13a^{crRNA}).

SUPPLEMENTARY MATERIALS

science.sciencemag.org/content/369/6499/54/suppl/DC1
Materials and Methods
Figs. S1 to S12
Tables S1 to S7
References (*31–44*)
MDAR Reproducibility Checklist

View/request a protocol for this paper from *Bio-protocol*.

6 March 2020; accepted 15 May 2020
Published online 28 May 2020
10.1126/science.abb6151

Science

A phage-encoded anti-CRISPR enables complete evasion of type VI-A CRISPR-Cas immunity

Alexander J. Meeske, Ning Jia, Alice K. Cassel, Albina Kozlova, Jingqiu Liao, Martin Wiedmann, Dinshaw J. Patel and Luciano A. Marraffini

Science **369** (6499), 54-59.
DOI: 10.1126/science.abb6151originally published online May 28, 2020

An infallible inhibitor of Cas13

CRISPR-Cas13 protects bacterial populations from viral infections by indiscriminately destroying the RNA of the cell and its invader, simultaneously arresting the growth of infected hosts and the spread of the virus. This response is mediated by the Cas13 nuclease, which unleashes massive RNA degradation after recognition of viral transcripts that are complementary to its guide RNA. Meeske *et al.* discovered AcrVIA1, a viral-encoded inhibitor that binds to Cas13 to occlude the RNA guide and prevent the activation of the nuclease (see the Perspective by Barrangou and Sontheimer). As opposed to inhibitors of DNA-cleaving CRISPR-Cas systems, which require multiple infections to neutralize all Cas nucleases of the host, production of AcrVIA1 by a single virus is sufficient to overcome the CRISPR-Cas13 response.

Science, this issue p. 54; see also p. 31